

Ultrashallow junctions in Si using decaborane? A molecular dynamics simulation study

Roger Smith^{a)} and Marcus Shaw

Department of Mathematical Sciences, Loughborough University, Leicestershire LE11 3TU, United Kingdom

Roger P. Webb

Department of Electronic and Electrical Engineering, University of Surrey, Guildford GU2 5XH, United Kingdom

Majeed A. Foad

Applied Materials, Foundry Lane, Horsham, West Sussex RH13 5PY, United Kingdom

(Received 4 September 1997; accepted for publication 2 December 1997)

The feasibility of using decaborane $B_{10}H_{14}$, for the manufacture of shallow junctions in Si is investigated by means of molecular dynamics simulations. Bombardment energies of 1, 2, and 4 keV are investigated and the simulations run for up to 7 ps in order to ascertain the implantation profiles of the B atoms, the whereabouts of the H from the impacted molecule and the damage to the lattice. The simulations show that if a small binding energy of the B atom in the Si lattice is assumed then most of the B from the cluster is implanted. The implantation distributions are flatter with depth than those for single B interactions and the surface layers undergo damage and amorphisation in the proximity of the impact. © 1998 American Institute of Physics.

[S0021-8979(98)03706-2]

I. INTRODUCTION

As silicon chips become even faster, ultrashallow junctions at depths of less than 100 nm will be required.¹ To implant B atoms to these depths by conventional ion implantation is quite difficult. The acceleration voltage of the B ions can be <1 keV and at these voltages space-charge blow up of the beam causes a drastic reduction in the beam current. This has led to the development of deceleration techniques where ion beams are extracted, mass analyzed and transported at relatively high energy then decelerated before implanting into silicon.² Recently, an alternative approach has been proposed using boron clusters.³ If the cluster were to contain n -boron atoms, the potential advantage is that only one charge per cluster is required to accelerate n -B atoms. In addition and for shallow junction applications, clusters can be transported at relatively high energy with the result of low impact energy per boron atom. Space-charge blow up of the beam can therefore be minimized and more B atoms implanted for the same beam current. Another potential advantage of using clusters is that the energy deposition in the crystal will tend to be localised near the surface with less channeling by individual B ions. Such channelling can occur even at low energies.⁴ The use of decaborane has been proposed as a possible means to implant B close to a silicon surface.⁵ The decaborane molecule is a member of a family of around thirty boron hydrides⁶ but the advantage of this particular B cluster is that it contains a relatively large number (10) of B atoms and it is also less toxic than some other B_xH_y compounds such as diborane or pentaborane. The molecule is shown schematically in Fig. 1. It is not especially

symmetric but in general terms it can be seen that the B atoms can be thought of as forming the central part of the cluster with the H atoms bonded external to this central region. The B–B bonds range between 1.71 and 2.0 Å and the B–H bonds range from 1.2 to 1.3 Å.

In this article we describe the results of molecular dynamics (MD) computer simulations of the effect of the interaction of the decaborane molecule with the dimer reconstructed Si{100} (2×1) surface. Interaction energies of 1, 2, and 4 keV are chosen for the study. The implantation profiles of the B atoms will be the primary focus of the study but also considered is the particle ejection from and damage to the Si lattice and the effect of the H atoms on the process.

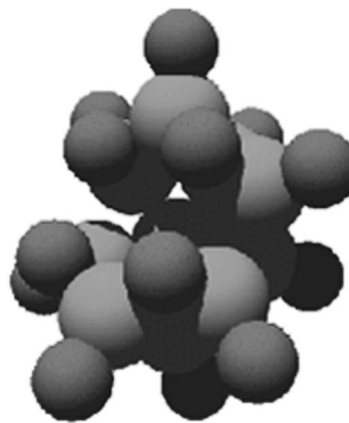


FIG. 1. A schematic representation of the decaborane molecule. The lighter coloured larger atoms are B, the small atoms H.

^{a)}Electronic mail: r.smith@lboro.ac.uk

TABLE I. The parameters for the pairwise Si–B potential function. For $r < 1.1 \text{ \AA}$, the ZBL (Ref. 7) potential is used. For $1.1 \text{ \AA} < r < 1.8 \text{ \AA}$, the potential is given by the splining function $V = \exp(f_1 + f_2 r + f_3 r^2 + f_4 r^4)$ (measured in electron volts). For $r > 1.8 \text{ \AA}$, the Morse interaction potential $D_e \{ \exp[-2\beta(r-r_e)] - 2 \exp[-\beta(r-r_e)] \}$ is used. Throughout the interatomic separation is calculated in \AA 's.

f_1	f_2	f_3	f_4	D_e (eV)	β	r_e (\AA)
14.30657	-25.74345	21.18573	-6.58849	0.25	1.5	2.351

II. METHODOLOGY

A. Interaction potentials

We investigated two interaction models between the B and the Si atoms. The short-ranged Si–H interactions were modelled using the ZBL screened Coulomb potential,⁷ joined smoothly to the Murty–Atwater potential.^{8,9} The Murty–Atwater potential is a modification to the Si Tersoff potential,¹⁰ which models well many of the small Si–H cluster and surface properties. There is also some agreement with *ab initio* calculations of H interstitials but generally the short-ranged nature of the Si–H potential which cuts off at 2 \AA oversimplifies some of this description. Reference 8 describes the static properties of this potential in more detail. To obtain a good description of the B–H and B–Si interactions is more problematical. Many previous MD simulations of B implantation into Si^{4,11} have used only the ZBL repulsive interaction between the B and the Si this is clearly a gross oversimplification since it is known that the B often takes up a substitutional site within the Si lattice and must have some weak binding to the lattice. High-energy MD simulations can very accurately predict the range profiles of B in Si using this approximation¹¹ but it is by no means clear that this will be sufficient for shallow implants. We therefore investigate two models for the B–Si interactions. The first model uses only the ZBL part. The second assumes that the ZBL potential is joined to a pairwise Morse potential which has a minimum at the nearest-neighbor spacing of the Si atoms in the lattice and a dimer binding energy of 0.25 eV. The effect is to make the substitutional site in Si a favorable position but with a relatively weak bonding of around 1 eV. Since this potential has not previously been reported the parameters are given in Table I.

The B–B and B–H interactions are also assumed to be entirely repulsive and modelled by the ZBL potential. However, in this case the potential is assumed to be very short ranged, cutting off at 1.16 \AA for the B–H and at 1.5 \AA for

B–B. This is a weakness of the model for low-energy interactions because it means that there is no interaction between any of the atoms in the decaborane cluster which is therefore destroyed completely on impact with the surface with no fragmentation into smaller clusters possible. At the energies considered here this approximation is expected to have a marginal effect on the range profiles because the binding energy per atom in the decaborane molecule is still much less than the kinetic energy of impact.

B. MD simulation

The crystal sizes used for the simulations were chosen to be large enough to contain the cascade resulting from the impact. For the 1 keV interaction, a rectangular crystal $85 \text{ \AA} \times 65 \text{ \AA} \times 85 \text{ \AA}$, containing 22 552 atoms was chosen. For 2 keV, the dimensions were $100 \text{ \AA} \times 80 \text{ \AA} \times 100 \text{ \AA}$, containing 38 904 atoms and, finally for 4 keV, a crystal size of $115 \text{ \AA} \times 90 \text{ \AA} \times 115 \text{ \AA}$, containing 63 912 atoms was used. The y direction was taken to be perpendicular to the surface and periodic boundary conditions were taken in the x and z directions. Thermal vibrations of the lattice were ignored. A fixed timestep of 0.2 fs was chosen and the simulations run for 7 ps. For the largest crystal, this resulted in a few days computing on a Sun Ultrasparc computer. The kinetic energy of interaction is shared between the atoms in the decaborane cluster in such a way that all are approaching the surface at the same speed. Thus, for example, in a 2 keV impact the B atoms would each have a kinetic energy of 177 eV and the H atoms 16.5 eV. Rotational and internal vibrational energy were not taken into account in the model since there was no assumed interaction between the atoms in the decaborane cluster. A random orientation of the molecule was assumed before each impact and a variety of impact points were chosen randomly near the centre of the crystal. The uncharged molecule shown in Fig. 1 has an approximately spherical shape but it is unclear that this shape will be maintained in the charged state. The lack of internal binding energy in the simulated molecule means that any analysis of orientation effects on the implantation profiles could be over-rigorous compared to this other approximation in the model. A more detailed study including binding and molecular shape and orientation will be carried out after this preliminary study.

TABLE II. The mean depth of the implanting species 7 ps after impact together with the amount of material implanted. All data are an average of 10 molecular impacts. The mean ranges for B and H exclude the adatoms and the channelled particles.

Atom	1 keV ^a	1 keV	2 keV ^a	2 keV	4 keV
H mean depth range	9.4 \AA	10.3 \AA	15.0 \AA	14.6 \AA	19.4 \AA
B mean depth range	11.5 \AA	11.7 \AA	19.1 \AA	16.3 \AA	28.3 \AA
% of H implanted	43%	49%	41%	49%	47%
% of H adatoms	11%	9%	11%	7%	3%
% of B implanted	29%	88%	59%	86%	96%

^aNo binding.

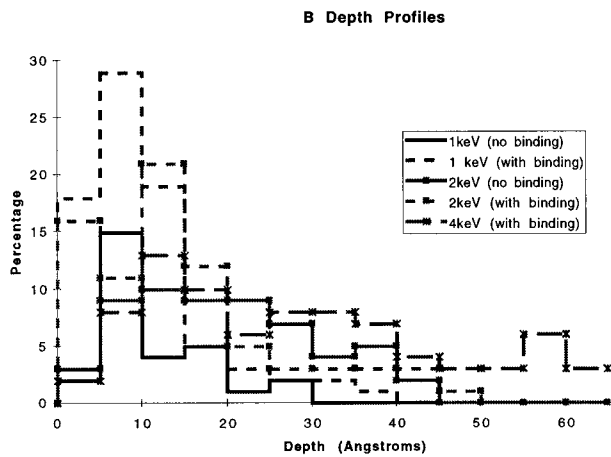


FIG. 2. The B implantation profiles.

III. RESULTS

A. B and H depth distributions

The binding energy of the B to the Si crystal turned out to be an important factor in determining the amount of B implanted into the crystal. Table II shows that without the inclusion of this binding energy term 71% of the boron either was ejected or diffused out of the lattice at an impact energy of 1 keV, whereas 88% stayed in the lattice with the binding term included. As can also be seen from the table, the corresponding figures for the 2 keV impacts were 59% of B implanting without the binding energy term and 86% with this term included. In all cases the bombardment energy refers to that of the full molecule. At 4 keV with binding 96% of the B atoms implanted into the crystal. At 1 keV the average range of the B atoms was approximately the same with or without the binding term, viz 11.5 Å as opposed to 11.7 Å but at 2 keV the range is 2.8 Å less with the binding term included. However, the average range is not an especially useful quantity because the implantation distributions have tails which are relatively long. At 1 keV the B implantation distribution peaks at between 5 and 10 Å, whereas this increases to between 10 and 15 Å at 2 and 4 keV. At 4 keV Fig. 2 shows that the distribution is much flatter with a much

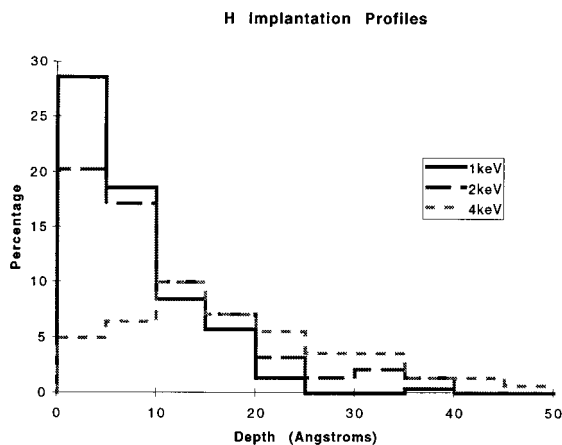


FIG. 3. The combined H implantation profiles.

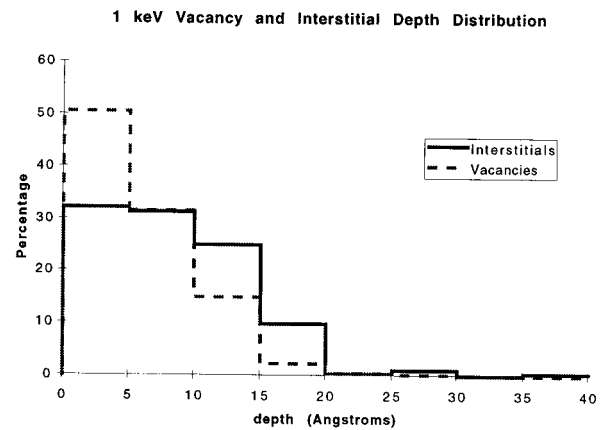


FIG. 4. The 1 keV vacancy and interstitial depth distribution.

longer tail than at 2 keV. In addition 10% of the B atoms channelled to depths >90 Å which was the depth of the crystal used in our simulations. At energies lower than 4 keV no B atoms channelled. Without the inclusion of the binding energy term some of the near-surface B diffused out of the crystal. An analysis of the data shows that near-surface B atoms are quite mobile in the absence of the binding energy term and some of these atoms can diffuse out of the crystal throughout the length of the simulations which were run for 7 ps. This causes a reduction in the number of B atoms just below the surface in the no Si-B binding case.

The effect of B-Si binding on the H implantation profiles is much less. There is some indication that more H is implanted with the B-Si binding energy term included and slightly less in the form of adatoms on the surface. However, the H distributions with or without Si-B binding were approximately the same to the statistical accuracy of the calculation. The combined results are given in Fig. 3. At 1 and 2 keV the H peak was at the surface due to a relatively large number of H adatoms. Table II shows that the number of H adatoms decreases with energy and at 4 keV the H implantation distribution peaks at between 10 and 15 Å with a long tail to the distribution. Approximately 2% of H ions channel to depths greater than 90 Å at 4 keV.

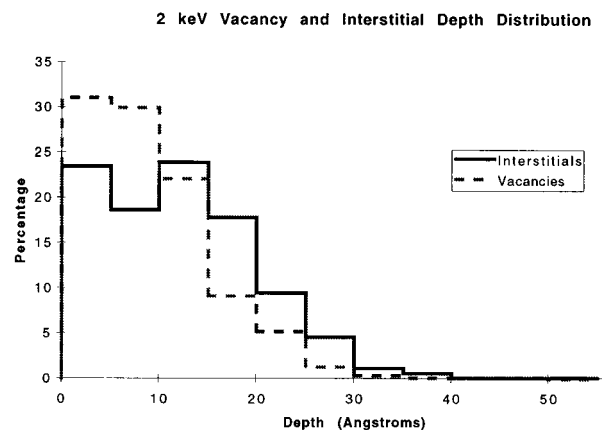


FIG. 5. The 2 keV vacancy and interstitial depth distribution.

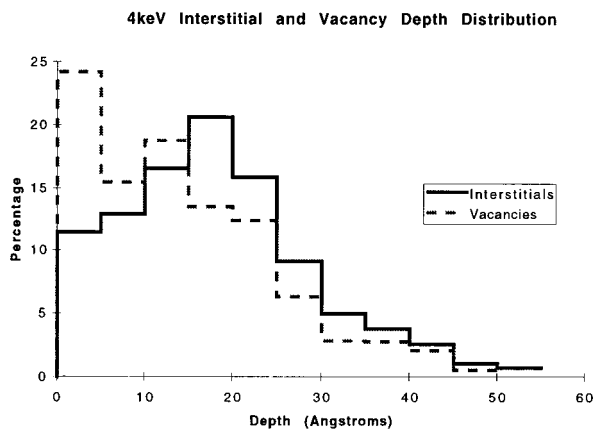


FIG. 6. The 4 keV vacancy and interstitial depth distribution.

Table II also shows that the amount of retained H within the crystal decreases with increasing energy. This is contrary to what might be expected for single H impacts where the penetration probability will decrease with decreasing energy. What seems to be the case here is that the initial densification at the impact, which increases with increasing impact energy, reduces the penetration probability for the H. The B atoms have a greater momentum than the H atoms and are able to penetrate this region.

B. Sputtering yields

The calculated sputtering yields as a result of the molecular impact are low and we could detect no statistically significant dependence of sputtering yields on the B–Si binding. The approximate sputtering yields (with a $\pm 30\%$ error margin) are 0.2 per molecular impact at 1 keV and 0.6 per molecular impact at 2 keV and 1.3 per molecular impact at 4 keV. In the 4 keV case one of the impacts ejected 6 Si atoms which was largely responsible for the increase over the value for 2 keV. Clearly better statistics are required to draw any definite conclusions regarding absolute yield values. Even if the statistics are good, in general experimental sputtering yields are generally not especially accurately simulated using MD. However previous results for calculations of Ar impacts on the Si{100} (2×1) surface have been encouragingly close to measured values from amorphous silicon.¹² The results calculated here at least give some general trends.

C. Damage to the crystal and the defect distribution

There is no absolute criterion in an atomistic simulation of the definition of a vacancy or an interstitial. In previous work on metals¹³ atoms which are within a predefined distance of a lattice site are assumed to recombine to that site after the simulation is terminated. It is usual to take a figure of between a third and half of the nearest-neighbor spacing for this distance when dealing with metals. However, Si amorphises more easily than metals because of the covalent bonding and the relatively wide open spaces in the lattice. As a result we have chosen a bigger recombination distance of 1.75 Å. This value gives approximately the same number of defects as would be expected at 1 keV using the Kinchin–

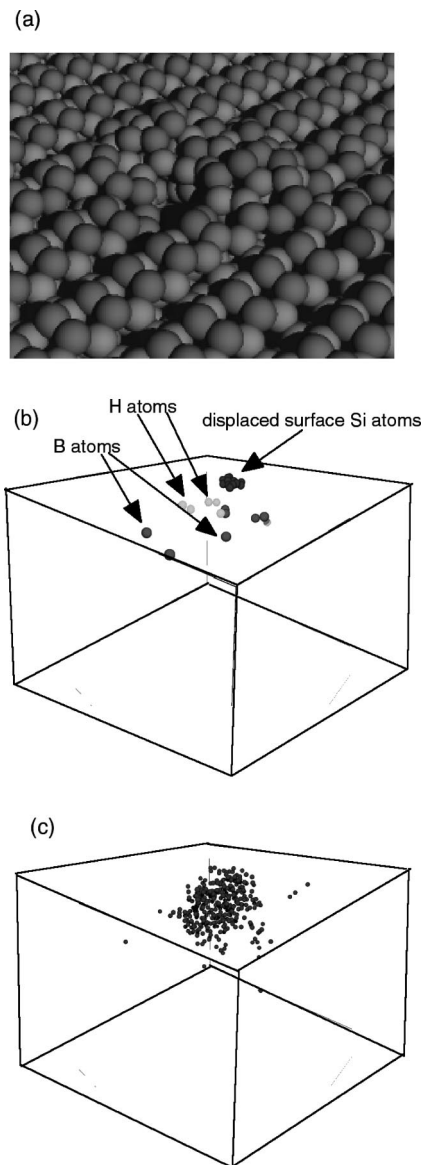


FIG. 7. Radiation damage after impact by a (a) 4 keV decaborane molecule surface damage. Note the surface swelling adjacent to a small crater (b) The crystal drawn from a different perspective where only the adatoms and implanted atoms are shown. (c) The distribution of the interstitial Si atoms. In (b) and (c) the crystal surface is $115 \text{ \AA} \times 115 \text{ \AA}$.

Pease formula. The depth distributions of the vacancies and interstitials are shown in Figs. 4 to 6. Only data for the case of Si–B binding are shown here. At all energies from 1 to 4 keV the vacancy distribution peaks at the surface. This is because often a small crater forms near the impact region of the decaborane molecule. Figure 7 shows an example of the distribution to the surface at 4 keV where both a small crater and a swelling of the surface coexist adjacent to the crater. This is partly due to the amorphisation induced by the radiation damage but also because of the net increase in the number of particles within the lattice, in this case 10 B and 6 H atoms. Also shown in Fig. 8 is an example of the surface damage caused by a 2 keV impact. Two H adatoms are clearly visible.

At 4 keV the interstitial distribution peaks at between 15 and 20 Å, whereas the vacancy distribution (excluding the

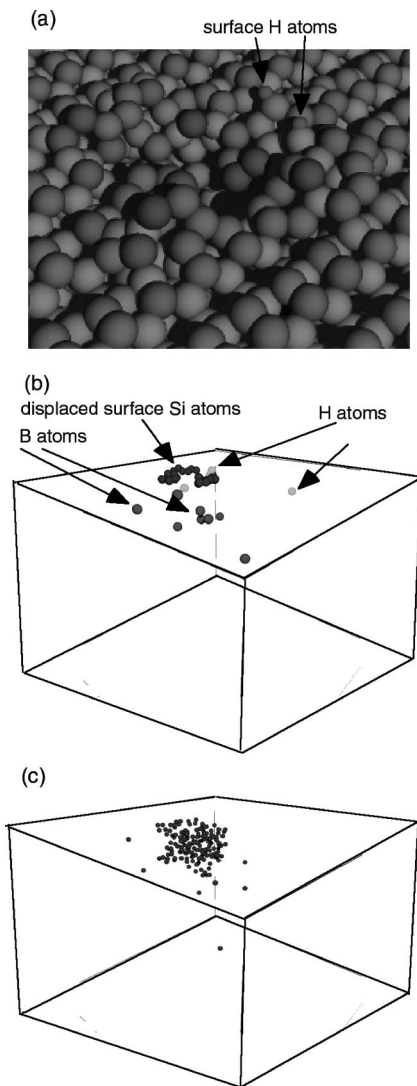


FIG. 8. Radiation damage after impact by a 2 keV decaborane molecule. (a) The surface damage close to the impact point of the cluster. Note the two H adatoms. (b) The crystal drawn from a different perspective where only the adatoms and implanted atoms are shown. (c) The distribution of the interstitial Si atoms. In (b) and (c) the crystal surface is $115 \text{ \AA} \times 115 \text{ \AA}$. The spatial distribution of B atoms shown above is typical of a number of trajectories. The impact itself does not cause sufficient dispersion of the B atoms to produce the correct B density within the Si crystal for semiconductor applications.

surface region) peaks at between 10 and 15 \AA , i.e., approximately 1 lattice unit closer to the surface. The number of defects per impact increases approximately as the square of the impact energy from 51 at 1 keV to 107 at 2 keV to 171

at 4 keV. However, the 4 keV results are an underestimate since 10 B atoms and 3 H atoms channelled out of the bottom of the crystal and these would undoubtedly cause further damage at greater depths as they eventually slow. The amount of energy unaccounted for in this way is about 280 eV per impact. It thus appears that for these molecular impacts over this energy range that the induced damage is more nearly proportional to the impact energy in agreement with the Kinchin–Pease formula for single particle impact in the absence of a surface.

IV. CONCLUSION

The simulations appear to demonstrate that low-energy implantation of B atoms into Si should be feasible using decaborane. However, to determine the efficiency of the process using MD computer simulation requires a better description of the interatomic forces between B and Si as the amount of B implanted is critically dependent on this parameter. The simulations also show that some H is also implanted. Although the amount is less than the B since a large amount of H is reflected from the crystal, this must be taken into account when assessing the electronic properties of the modified crystal. Finally, it should be noted that both small craters and local swelling of the surface results from individual molecular collisions. For deeper implantation, a damaged surface may not be so much of a problem but for ultrashallow junctions the effect of a damaged surface needs to be assessed before devices manufactured using decaborane implantation can be routinely used.

¹National Technology Road Map for Semiconductors, Semiconductor Industry Association, San Jose, California, 1997.

²M. A. Foad, J. England, S. Moffatt, and D. G. Armour, Paper presented at Ion Implantation Technology '96, Austin Texas, June 1996.

³I. Yamada, W. L. Brown, J. A. Northby, and M. Sosnowski, Nucl. Instrum. Methods Phys. Res. B **79**, 223 (1993).

⁴R. Smith and R. P. Webb, Philos. Mag. Lett. **64**, 253 (1991).

⁵K. Goto, J. Matsuo, D. Takeuchi, T. Sugii, H. Minikata, and I. Yamada, in *Application of Accelerators in Research and Industry*, edited by J. L. Duggan and I. L. Morgan (AIP, New York, 1997), pp 937–940.

⁶W. N. Lipscomb, *Boron Hydrides*, Benjamin (1963).

⁷J. F. Ziegler, J. P. Biersack, and U. Littmark, *The Stopping and Ranges of Ions in Solids* (Pergamon, New York, 1985).

⁸M. V. R. Murty and H. A. Atwater, Phys. Rev. B **51**, 4889 (1995).

⁹K. M. Beardmore and R. Smith, Philos. Mag. A **74**, 1439 (1996).

¹⁰J. Tersoff, Phys. Rev. Lett. **56**, 632 (1986); **61**, 2879 (1988); Phys. Rev. B **39**, 5566 (1989).

¹¹K. M. Beardmore, D. Cai, and N. Gronbech-Jensen, IEEE 96TH8182, 535 (1997).

¹²R. Smith, *Atom and Ion Collisions in Solids and at Surfaces* (Cambridge University Press, Cambridge, England, 1997).

¹³R. Smith, B. V. King, and K. M. Beardmore, Radiat. Eff. Defects Solids **141**, 425 (1997).